

# Dynamic Energy Dispatch in Isolated Microgrids Based on Deep Reinforcement Learning

Lei Lei *Senior Member, IEEE*, Yue Tan, Glenn Dahlenburg, Wei Xiang *Senior Member, IEEE*, Kan Zheng *Senior Member, IEEE*

**Abstract**—This paper focuses on deep reinforcement learning (DRL)-based energy dispatch for isolated microgrids (MGs) with diesel generators (DGs), photovoltaic (PV) panels, and a battery. A finite-horizon Partial Observable Markov Decision Process (POMDP) model is formulated and solved by learning from historical data to capture the uncertainty in future electricity consumption and renewable power generation. In order to deal with the instability problem of DRL algorithms and unique characteristics of finite-horizon models, two novel DRL algorithms, namely, FH-DDPG and FH-RDPG, are proposed to derive energy dispatch policies with and without fully observable state information. A case study using real isolated microgrid data is performed, where the performance of the proposed algorithms are compared with the myopic algorithm as well as other baseline DRL algorithms. Moreover, the impact of uncertainties on MG performance is decoupled into two levels and evaluated respectively.

**Index Terms**—Microgrid; Energy Management; Deep Reinforcement Learning

## I. INTRODUCTION

Microgrids (MGs) are small-scale, self-supporting power networks driven by on-site generation sources. They can potentially integrate renewable energy sources (RESs) such as solar and wind, as well as energy storage elements such as electrochemical battery, and often use a base load generation source such as reciprocating diesel engines of heavy fuel oil. An MG can either connect or disconnect from the external main grid to operate in grid-connected or isolated-mode. MGs improve grid reliability and supply sustainable and quality electric power. However, their planning and operations are faced with challenges from uncertainty because of the difficulty in accurate prediction of future electricity consumption and renewable power generation. As RESs reach high levels of grid penetration, intelligent energy management that can handle variability and uncertainty becomes essential for an MG to provide reliable power supply efficiently.

In this paper, we focus on an isolated MG system including diesel generators (DGs), photovoltaic (PV) and a battery. Such systems can be found in many remote areas all over the world, which are inefficient to connect to the main grid. As the MGs in remote locations usually lack advanced control hardware, we do not consider controllable load for demand side management. However, a load bank is used at the power station to protect the DGs, so that excessive DG power can be dissipated to avoid curtailing the generation. We consider the DGs as the primary source of power, while the PV acts as a clean complementary power source. Our main objective is to manage the energy dispatch of the DGs so that their

operational cost can be minimized by fully exploiting the PV power, while satisfying the critical requirement to maintain balance between power generation and consumption. The main challenge stems from the unpredictability in future PV generation and load demand, making it difficult to maintain balance between power generation and consumption without inefficient operations of the DGs.

The battery can help overcome the above challenge to some extent, as it can charge or discharge to compensate for short-term unbalance. Moreover, the battery can act as an additional power source to minimize operational cost of DGs. However, the battery also brings new challenges in energy management. As the maximum amount of energy that can be charged or discharged at a certain point of time is limited by the energy storage capability and the current state-of-charge (SoC) of the battery, while the current SoC is in turn determined by the previous charging/discharging behavior, energy management becomes a sequential decision problem for a dynamic system where earlier decisions influence future available choices. Therefore, dynamic optimization techniques are required to optimize the overall performance over a finite time horizon instead of only the instantaneous performance at a single point of time.

### A. Related Work

1) *Energy Management Approaches in MG*: Several approaches to dealing with uncertainties have been adopted for energy management in microgrids by recent works, such as *Stochastic Optimization (SO)* [1]–[3], *Robust Optimization (RO)* [4], [5], *Model Predictive Control (MPC)/Receding Horizon Control (RHC)* [6]–[9], *Approximate Dynamic Programming (ADP)* [10]–[12], and *Lyapunov Optimization* [13], [14].

The *SO* and *RO* based approaches do not consider the sequential decision problem. In *MPC/RHC*, the optimal control problem for a dynamic system is considered, where the system states evolve dynamically over time. At each time step, a sequence of optimal control actions is computed by solving an open-loop deterministic optimization problem for the prediction horizon, but only the first value of the computed control sequence is implemented. This process is iteratively repeated, and a prediction model of the dynamic system behavior is required. In [6], the *MPC* technique is applied to determine the unit commitment and optimal power flow problems in an isolated MG, where the stochastic variables are assumed to be perfectly predicted. As the performance of the *MPC* based approaches heavily depends on the accuracy of the prediction

model, a stochastic *MPC* method is adopted in [7] to optimally dispatch energy storage and generation, where the uncertain variables are treated as random processes. In [8], an *MPC* strategy for isolated MGs in rural areas is developed, where the first stage derives the optimal power dispatch based on real-time predication of future power profiles, while the second stage adjusts the DG power to improve the robustness of the control strategy toward prediction errors. In [9], *RO* and *RHC* are combined to manage forecasting errors in energy management of isolated microgrids.

*Dynamic Programming (DP)* normally considers stochastic optimal control problems, where the system states evolve over time in a stochastic manner. The optimal control action under each system state needs to be determined to optimize the expected performance over a time horizon. The stochastic evolution of the state-action pair over time forms a Markov Decision Process (MDP). The expected performance of a MDP starting from a certain system state is referred to as the value function of the specific state. *DP* is a model-based control technique similar to *MPC*, which requires the transition probabilities of the MDP model to be available. One important challenge in *DP* is the curse-of-dimensionality problem, where the state space of the MDP model is too large to derive solutions within a reasonable period of time. Therefore, *ADP* is widely adopted as an efficient method to overcome this challenge by approximating the value functions. In [10], an *ADP* based approach is developed to derive real-time energy dispatch of an MG, where the value functions are learned through neural networks. A near optimal policy is obtained through the approximate policy iteration algorithm. In [11], [12], the optimal operation of MG is formulated as a stochastic mixed-integer nonlinear programming (MINLP) problem, and *ADP* is applied to decompose the original multi-time-period MINLP problem into single-time period nonlinear programming problems.

2) *Deep Reinforcement Learning*: In the above papers, the stochastic variables and processes are either assumed to be available by prediction models or represented by their corresponding expected values. On the other hand, Reinforcement Learning (RL) provides model-free methods to solve the optimal control problems of dynamic systems without requiring the stochastic properties of the underlying MDP model [15]. When combined with Deep Learning (DL), the more powerful Deep Reinforcement Learning (DRL) methods can deal with the curse-of-dimensionality problem by approximating the value functions as well as policy functions using deep neural networks [16].

RL/DRL algorithms can be broadly classified into value-based method, such as DQN [17] and Double DQN [18]; Monte Carlo policy gradient method, such as REINFORCE [19]; and actor-critic method, such as Deep Deterministic Policy Gradient (DDPG) [20], asynchronous Advantage Actor-Critic (A3C) [21], Trust Region Policy Optimization (TRPO) [22], Recurrent Deterministic Policy Gradients (RDPG) [23]. Actor-critic method combines the advantages of both value-based and Monte Carlo policy gradient methods. Compared with the Monte Carlo policy gradient method, it requires a far less number of samples to learn from and less computational

resources to select an action, especially when the action space is continuous. Compared with the value-based method, it can learn stochastic policies and solve RL problems with continuous actions. However, actor-critic method may be unstable due to the recursive use of value estimates.

Recent years have seen emerging applications of RL/DRL to provide energy management solutions for MGs [24]–[28]. In [24], a value-based DRL algorithm is proposed to optimally activating the energy storage devices, where three discrete actions are considered, i.e., discharge at full rate, keep it idle, charge at full rate. Value-based DRL algorithms are relatively simple, but it cannot deal with continuous actions that are common in energy management problems. In [25], an evolutionary adaptive dynamic programming and reinforcement learning framework is introduced to develop an intelligent dynamic energy management system for a smart MG. The proposed solution has a similar architecture to that of actor-critic DRL algorithms. In [26], a multi-agent-based RL model is used to study distributed energy management in an MG. Considering the existence of model uncertainty and parameter constraints, a DDPG-based DRL algorithm is proposed in [27] to solve the energy management problem for smart home. In [28], the authors focus on MG-enabled multi-access edge computing networks and formulate the energy supply plan problem into MDP, which is solved by the proposed DRL-based approach.

## B. Contributions

In this paper, we formulate a finite-horizon Partial Observable Markov Decision Process (POMDP) model for the energy dispatch of DGs in isolated MGs. For comparison purpose, we also formulate a finite-horizon MDP model to study the impact of uncertainty on system performance. We focus on intra-day operation of the MG where the duration of one day is divided into multiple time steps. The energy dispatch decision for DGs is determined at the beginning a time step. The objective is to optimize the sum of performance over all the time steps within the time horizon, i.e., one day. Performance considered in the optimization problem includes: (1) supply the power requirements of customer loads at all times; (2) eliminate reverse power flow; (3) minimize power generation cost of DGs and maximize the utilization of renewable energy resource. Note that it is straightforward to adapt the proposed finite-horizon models to study intra-month and intra-year operations.

The main contributions of this paper lie in the following aspects:

- **DRL models that facilitate analyzing the impact of uncertainty**: In this paper, the proposed finite-horizon MDP and POMDP models enable one to analyze and address the impact of uncertainty on isolated MGs. Specifically, we divide the uncertainty into two time granularities: (1) uncertainty due to data variation between two consecutive time steps; (2) uncertainty due to data variation between two consecutive days. The “partial observable” and “finite-horizon” formulation of the DRL models help us to capture the two levels of uncertainty, respectively.
- **DRL algorithms that address the instability problem and finite-horizon setting**: DRL algorithms are known

to be unstable and hard to converge, and there are many challenges when applied to solve real-world problems [29]. Most of the well-known DRL algorithms such as DQN and DDPG are evaluated by their performance in learning to play games. Moreover, they are usually applied to solve infinite-horizon MDP problems. In this paper, we first design a DRL algorithm namely finite-horizon deep deterministic policy gradient (FH-DDPG) for finite-horizon MDP model based on a well-known DRL algorithm - DDPG. The instability problem and unique characteristics of finite-horizon setting are addressed using two key ideas - backward induction and time-dependent actors. Next, in order to address the partial observable problem, we develop a second DRL algorithm namely finite-horizon recurrent deterministic policy gradient (FH-RDPG) for finite-horizon POMDP model. Similar to RDPG, which is a well-known DRL algorithm specifically designed to work in the partial observable domain, FH-RDPG also incorporates a Long Short Term Memory (LSTM) layer, which is a widely adopted recurrent neural network architecture capable of capturing long term time dependencies. However, the overall workflow of the FH-RDPG algorithm is similar to that of the FH-DDPG algorithm, both of which are based on backward induction. We specifically define the history in the POMDP model for the MG environment to facilitate the implementation of the FH-RDPG algorithm. We demonstrate that the proposed DRL algorithms outperform the baseline DRL algorithms such as DDPG and RDPG by large margins and are much more stable for solving the energy management problem.

The remainder of the paper is organized as follows. The system model is introduced in Section II. Section III formulates the MDP and POMDP models, which are solved by the two proposed DRL algorithms introduced in Section IV. In Section V, the performance of the proposed algorithms are compared with those of other baseline algorithms by simulation, where the results are analyzed and discussed. Section VI concludes the paper.

## II. SYSTEM MODEL

We consider an isolated MG system which consists of DGs, several PV panels, an electrochemical battery for energy storage, loads, and a load bank as shown in Fig. 1. The intra-day operation of the MG is divided into  $T$  time steps, indexed by  $\{1, \dots, T\}$ . The interval for each time step is  $\Delta t$ .

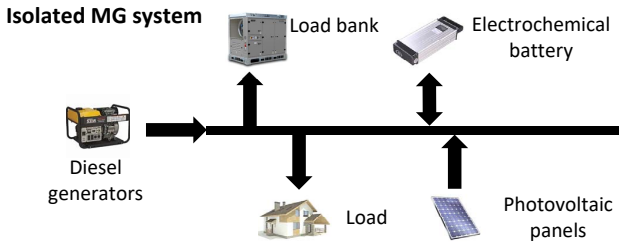


Fig. 1. Schematic of an isolated MG system.

### A. Diesel Generator Model

We consider there are  $D$  DGs ( $DG_1, \dots, DG_D$ ). Let  $P_t^{DG_d}$  denote the output power of the  $d$ -th DG  $DG_d$ ,  $\forall d \in \{1, \dots, D\}$ , at time step  $t$ . The operational constraints are given by

$$P_{\min}^{DG_d} \leq P_t^{DG_d} \leq P_{\max}^{DG_d}, \forall d \in \{1, \dots, D\}, \quad (1)$$

where  $P_{\min}^{DG_d}$  and  $P_{\max}^{DG_d}$  are the minimum and maximum output powers of  $DG_d$ , respectively.

Let  $c_t^{DG_d}$  be the generation cost of  $DG_d$ , which can be derived by the conventional quadratic cost function

$$c_t^{DG_d} = [a_d(P_t^{DG_d})^2 + b_d P_t^{DG_d} + c_d] \Delta t, \forall d \in \{1, \dots, D\}, \quad (2)$$

where  $a_d$ ,  $b_d$ , and  $c_d$  are positive coefficients for  $DG_d$ .

### B. Battery Model

Let  $E_t$  denote the state of charge (SoC) of the battery at the beginning of time step  $t$ . Let  $P_t^E$  denote the charging or discharging power of the battery, and  $u_t$  indicate charging status, which is 1 if battery is charging and 0 otherwise.

The SoC of battery  $E_{t+1}$  at time step  $t+1$  can be derived based on the SoC  $E_t$  at time step  $t$  as

$$E_{t+1} = E_t + \eta_{\text{ch}} u_t P_t^E \Delta t - (1 - u_t) P_t^E \Delta t / \eta_{\text{dis}}, \quad (3)$$

where  $\eta_{\text{ch}}$  and  $\eta_{\text{dis}}$  are the charging and discharging efficiencies of the battery.

In order to determine  $P_t^E$  and  $u_t$ , we define the following variable

$$\delta_t = \sum_{d=1}^D P_t^{DG_d} + P_t^{\text{PV}} - P_t^{\text{L}}, \quad (4)$$

where  $P_t^{\text{PV}}$  and  $P_t^{\text{L}}$  are the aggregated PV output power and load power demand at time step  $t$ , respectively.

Therefore, we can set

$$u_t = \begin{cases} 1, & \text{if } \delta_t \geq 0 \\ 0, & \text{if } \delta_t < 0 \end{cases}, \quad (5)$$

and

$$P_t^E = \begin{cases} \min(\delta_t, P_{\text{ch\_lim}}^E), & \text{if } \delta_t \geq 0 \\ \min(-\delta_t, P_{\text{dis\_lim}}^E), & \text{if } \delta_t < 0 \end{cases}, \quad (6)$$

where

$$P_{\text{ch\_lim}}^E = \min(P_{\text{max}}^E, (E_{\text{max}} - E_t) / (\eta_{\text{ch}} \Delta t)), \quad (7)$$

and

$$P_{\text{dis\_lim}}^E = \min(P_{\text{max}}^E, \eta_{\text{dis}}(E_t - E_{\text{min}}) / \Delta t), \quad (8)$$

are the battery charging and discharging power limit.  $E_{\text{max}}$  and  $E_{\text{min}}$  are the maximum and minimum energy level of the battery, and  $P_{\text{max}}^E$  is the maximum charging or discharging power.

If  $\delta_t > 0$ , the generation is larger than demand, the excessive power will be charged to the battery. However, if  $\delta_t > P_{\text{ch\_lim}}^E$ , the excessive power beyond the charging capability of the battery will go to the load bank, which will be lost or generation will be curtailed. If  $\delta_t < 0$ , the generation is smaller than demand, the battery needs to be discharged to supply the load. However, if  $-\delta_t > P_{\text{dis\_lim}}^E$ , even the battery cannot provide enough power, which will see part of the load unserved.

### III. MDP AND POMDP MODELS

In this section, we shall formulate a finite-horizon POMDP problem to minimize the power generation cost as well as the power demand and generation unbalance, where the fluctuating loads and stochastic generation of PV panels are taken into account. In order to analyze the impact of uncertainty on system performance, we also formulate a corresponding finite-horizon MDP problem for comparison purpose.

#### A. State and Observation

We define the system state at time step  $t$ ,  $\forall t \in \{1, 2, \dots, T\}$ , as  $s_t = (P_t^L, P_t^{PV}, E_t)$ . Let  $s_{lp,t} = (P_t^L, P_t^{PV})$  and  $s_{e,t} = E_t$ , we have  $s_t = (s_{lp,t}, s_{e,t})$ .

Due to the uncertainties of future load and renewable power generation, the agent is unable to observe  $P_t^L$  and  $P_t^{PV}$  at the beginning of time step  $t$ . Instead, it receives observation  $o_t$  of the system at the beginning of time step  $t$ , where we define the observation as  $o_t = (P_{t-1}^L, P_{t-1}^{PV}, E_t)$ . Note that  $P_{t-1}^L$  and  $P_{t-1}^{PV}$  are the aggregated power demand of loads and power output of PV at time step  $t-1$ , respectively, which are readily available to the agent at the beginning of time step  $t$ . Let  $o_{lp,t} = (P_{t-1}^L, P_{t-1}^{PV})$  and we have  $o_t = (o_{lp,t}, s_{e,t})$ . Note that  $o_{lp,t} = s_{lp,t-1}$ .

The state space and observation space  $\mathcal{S} = \mathcal{O} = [P_{\min}^L, P_{\max}^L] \times [P_{\min}^{PV}, P_{\max}^{PV}] \times [E_{\min}, E_{\max}]$ , where  $P_{\min}^L$  and  $P_{\max}^L$  are the minimum and maximum aggregated loads, while  $P_{\min}^{PV}$  and  $P_{\max}^{PV}$  are the minimum and maximum aggregated power outputs of PV.

#### B. Action

We define the action at time step  $t$ ,  $\forall t \in \{1, 2, \dots, T\}$ , as  $a_t = \{P_t^{DG_d}\}_{d=1}^D$ , which are the output power of DGs. The action space  $\mathcal{A} \in \bigcup_{d=1}^D [P_{\min}^{DG_d}, P_{\max}^{DG_d}]$ .

#### C. Policy

At time step  $t$ , the agent requires access to state  $s_t$  to determine the optimal action  $a_t$ , i.e.,  $a_t = \mu_t(s_t)$ , where  $\mu_t$  is a decision rule that prescribes a procedure for action selection at time step  $t \in \{1, \dots, T\}$ . The sequence of decision rules for all the time steps forms a policy  $\pi$ , i.e.,  $\pi = (\mu_1, \dots, \mu_T)$ . In the rest of this paper, we will refer to  $\mu_t, \forall t \in 1, \dots, T$  as a policy or policy function instead of a decision rule with a slight abuse of terminology.

**Remark 1 (Stationary and Non-Stationary Policy):** A policy is stationary if  $\mu_t = \mu$  for all  $t \in \{1, \dots, T\}$ , which are fundamental to the theory of infinite-horizon MDP [30]. On the other hand, the optimal policy for a finite-horizon MDP as studied in this paper is normally non-stationary [31]. This is because the value functions for the same system state are different at different time steps.

#### D. History

As only the observation  $o_t$  is available instead of  $s_t$ , the agent is provided with history  $h_t$  to derive action  $a_t = \mu_t(h_t)$ .

In a POMDP problem, the history is normally defined as  $h_t = (o_1, a_1, o_2, a_2, \dots, o_{t-1}, a_{t-1}, o_t)$ . In this paper, the

history provided to the agent is tailored for the MG energy management problem as below.

**Definition 1 (Definition of history):** We define history  $h_t = (o_{lp,t-\tau}, o_{lp,t-\tau+1}, \dots, o_{lp,t-1}, o_t)$ ,  $\forall t \in \{1, \dots, T\}$ , where  $\tau$  is the size of the past observation window.

Note that compared with the standard history definition, our definition does not include action history  $\{a_{t'}\}_{t'=t-\tau}^{t-1}$  nor battery SoC history  $\{s_{e,t'}\}_{t'=t-\tau}^{t-1}$  up to time step  $t-1$ . This is because we only need the historical load and PV generation data  $\{o_{lp,t'}\}_{t'=t-\tau}^{t-1}$  up to time step  $t-1$  to predict the load and PV state  $s_{lp,t}$  at time step  $t$ .

The evolution of history can be derived as

$$h_{t+1} = h_t \setminus \{s_{e,t}\} \cup \{o_{t+1}\} \quad (9)$$

#### E. Reward Function

The optimization objective is to minimize the total power generation cost and power unbalance in the MG within a 24-hour time horizon. Therefore, we define the reward function as

$$r_t(s_t, a_t) = -(k_1 \sum_{d=1}^D c_t^{DG_d} + k_2 c_t^{US}), \quad (10)$$

where  $k_1$  and  $k_2$  are weights indicating the relative importance of minimizing the power generation cost versus power unbalance.  $c_t^{DG_d}$  is given in (2), while  $c_t^{US}$  is the cost of the aggregated unserved or wasted active power, i.e.,

$$c_t^{US} = \begin{cases} k_{21}(\delta_t - P_{ch\_lim}^E)\Delta t, & \text{if } \delta_t > P_{ch\_lim}^E \\ -k_{22}(\delta_t + P_{dis\_lim}^E)\Delta t, & \text{if } \delta_t < -P_{dis\_lim}^E \\ 0, & \text{otherwise} \end{cases}, \quad (11)$$

where  $\delta_t$ ,  $P_{ch\_lim}^E$ , and  $P_{dis\_lim}^E$  are given in (4), (7), and (8), respectively.  $k_{21}$  and  $k_{22}$  are weights that indicate the relative importance of avoiding unserved power situation and wasted power situation.

#### F. Transition Probability

The state transition probability  $\Pr.(s_{t+1}|s_t, a_t)$  can be derived by

$$\Pr(s_{t+1}|s_t, a_t) = \Pr(P_{t+1}^L|P_t^L)\Pr(P_{t+1}^{PV}|P_t^{PV})\Pr(E_{t+1}|E_t, a_t), \quad (12)$$

where  $\Pr(E_{t+1}|E_t, a_t)$  is given in (3). However, the transition probabilities of the load power demands and PV power outputs, i.e.,  $\Pr(P_{t+1}^L|P_t^L)$  and  $\Pr(P_{t+1}^{PV}|P_t^{PV})$  are not available. We will use model-free reinforcement learning algorithms to learn the solution to the above POMDP problem based on real-world data.

#### G. Model Formulation

Given the above elements, if state  $s_t$  is considered to be known at each time step  $t$ , a finite-horizon MDP model can be formulated as

$$\max_{\mu} \sum_{t=1}^T E[r_t(s_t, \mu_t(s_t))]. \quad (13)$$

On the other hand, if only observation  $o_t$  instead of state  $s_t$  is considered to be known at each time step  $t$ , which is the practical case, the finite-horizon POMDP model can be formulated as

$$\max_{\mu} \sum_{t=1}^T \mathbb{E}[r_t(s_t, \mu_t(h_t))]. \quad (14)$$

Note that the expectations in (13) and (14) are taken w.r.t. the unique steady-state distribution induced by the given policy  $\pi = (\mu_1, \dots, \mu_T)$ .

**Remark 2 (Terminal Reward):** In a finite-horizon MDP, the reward  $r_T$  for the last time step is referred to as the terminal reward, which is normally considered to be independent of the action  $a_T$ . In the MDP and POMDP models formulated in this paper, the terminal reward is still dependent on action  $a_T$ , where the optimal action can be derived by a myopic policy, i.e.,  $\mu_T = \mu^{\text{mo}}$  that optimizes the terminal reward  $r_T$  without having to consider any future reward.

$\mu^{\text{mo}}$  can be derived directly without learning for the MDP model, but not for the POMDP model as the state information is not available.

#### IV. DRL ALGORITHMS

##### A. Algorithm for Finite-Horizon MDP: FH-DDPG

DRL algorithms are known to be unstable, and there are many challenges when applied to solve real-world problems [29]. Moreover, it is usually applied to solve infinite-horizon MDP problems. In this paper, we design a DRL algorithm for the formulated finite-horizon MDP model based on a baseline algorithm, i.e., DDPG. The instability problem and the unique characteristics of the finite-horizon setting are addressed using two key ideas as discussed below.

Firstly, in order to capture the time-varying policy  $\pi = (\mu_1, \dots, \mu_T)$  under a finite-horizon setting, we train  $T - 1$  actor networks  $\{\mu_t(s|\theta^{\mu_t})\}_{t=1}^{T-1}$  to approximate policy functions  $\{\mu_t(s)\}_{t=1}^{T-1}$ , instead of using only one actor network as in most up-to-date actor-critic algorithms. The policy  $\mu_T$  at the last time step  $T$  can be directly set to be the same as the myopic policy  $\mu^{\text{mo}}$ .

Secondly, in order to address the instability problem and achieve faster convergence, we use backward induction and divide the whole training process into training  $T - 1$  one-period MDPs in backward sequence, starting from time step  $T - 1$  and going backward to time step 1. In training the one-period MDP for each time step  $t \in \{T - 1, \dots, 1\}$ , DDPG is applied to derive the actor  $\mu_t(s|\theta^{\mu_t})$  along with a critic  $Q(s, a|\theta^Q)$ . Then, the actor weights are stored, and both the actor and critic trained for time step  $t$  are used as the target actor and critic for the previous time step  $t - 1$ , which is trained next in the proposed algorithm. In this way, we start by having the optimal policy for a single time step  $T$ , i.e.,  $\pi = (\mu_T(s) = \mu^{\text{mo}}(s))$  before training. And then, we derive the optimal policy starting from time step  $T - 1$  until the end of the time horizon after we train the one-period MDP for time step  $T - 1$ , i.e.,  $\pi = (\mu_{T-1}(s|\theta^{\mu_{T-1}}), \mu_T(s))$ . This process keeps going on until the training of the one-period MDP for time step 1 is finished, which gives us the complete

optimal policy starting from time step 1 until the end of the time horizon, i.e.,  $\pi = (\mu_1(s|\theta^{\mu_1}), \dots, \mu_{T-1}(s|\theta^{\mu_{T-1}}), \mu_T(s))$ . Note that DDPG is always used to solve the one-period MDPs in which an episode only consists of two time steps, and only the actor and critic of the first time step need to be trained. By greatly reducing the number of time steps within an episode, the performance of DDPG proves to be much more stable.

The proposed DRL algorithm for the finite-horizon MDP, namely FH-DDPG, is given in Algorithm 1.

---

##### Algorithm 1 FH-DDPG Algorithm

---

Randomly initialize actor network  $\mu(s|\theta^{\mu})$  and critic network  $Q(s, a|\theta^Q)$  with weights  $\theta^{\mu} = \theta^{\mu_0}$  and  $\theta^Q = \theta^{Q_0}$   
 Initialize target networks  $Q'$  and  $\mu'$  with  $\theta^{Q'} \leftarrow \theta^Q$  and  $\theta^{\mu'} \leftarrow \theta^{\mu}$

**for**  $t = T - 1, \dots, 1$  **do**

  Initialize replay buffer  $R$

  Initialize a random process  $\mathcal{N}$  for action exploration

**for** episode  $e = 1, \dots, M$  **do**

    Receive state  $s_t^{(e)}$

    Select action  $a_t^{(e)}$  according to the current policy and exploration noise

    Execute action  $a_t^{(e)}$  and observe reward  $r_t^{(e)}$  and observe new state  $s_{t+1}^{(e)}$

    Store transition  $(s_t^{(e)}, a_t^{(e)}, r_t^{(e)}, s_{t+1}^{(e)})$  in  $R$

    Sample a random minibatch of  $N$  transitions  $(s_t^{(i)}, a_t^{(i)}, r_t^{(i)}, s_{t+1}^{(i)})$  from  $R$

**if**  $t = T - 1$  **then**

      Set  $y_t^{(i)} = r_t^{(i)} + \gamma r_T(s_{t+1}^{(i)}, \mu^{\text{mo}}(s_{t+1}^{(i)}))$

**else**

      Set  $y_t^{(i)} = r_t^{(i)} + \gamma Q'(s_{t+1}^{(i)}, \mu'(s_{t+1}^{(i)}|\theta^{\mu'}))|\theta^{Q'}$

**end if**

    Update critic by minimizing the loss:

$$L = \frac{1}{N} \sum_i (y_t^{(i)} - Q(s_t^{(i)}, a_t^{(i)}|\theta^Q))^2$$

    Update the actor using the sampled policy gradient:

$$\nabla_{\theta^{\mu}} J \approx$$

$$\frac{1}{N} \left( \sum_i \nabla_a Q(s, a|\theta^Q)|_{s=s_t^{(i)}, a=\mu(s_t^{(i)})} \nabla_{\theta^{\mu}} \mu(s|\theta^{\mu})|_{s_t^{(i)}} \right)$$

**end for**

  update the target network:

$$\theta^{Q'} \leftarrow \theta^Q, \theta^{\mu'} \leftarrow \theta^{\mu}$$

  save weight of actor network:

$$\theta^{\mu_t} \leftarrow \theta^{\mu}$$

  Reset weight of actor and critic networks to initial value:

$$\theta^Q \leftarrow \theta^{Q_0}, \theta^{\mu} \leftarrow \theta^{\mu_0}$$

**end for**

---

### B. Algorithm for Finite-Horizon POMDP: FH-RDPG

The above FH-DDPG algorithm is designed to solve finite-horizon MDP problems. However in practice, the state information cannot be obtained at each time step. Therefore, in order to address the partial observable problem for finite-horizon POMDP, we propose another algorithm, namely FH-RDPG. In general, it is harder to use backward induction for solving POMDP as the history needs to be obtained first from Monte-Carlo simulation. However, in the MG environment under consideration in this paper, we can tackle this challenge by defining the history as given in Definition 1. Specifically, we only need the history data of the load and PV, i.e.,  $\{o_{lp,t'}\}_{t'=t-\tau}^t$  up to time step  $t-1$ , which can be obtained from real-world data without any need for simulation, to predict the load and PV state  $s_{lp,t}$  at time step  $t$ . On the other hand, the history action and battery SoC statistics that require simulation to obtain samples of trajectories are not needed to derive the optimal action for time step  $t$ .

The FH-RDPG Algorithm is given in Algorithm 2. Note that it is similar to the FH-DDPG algorithm except that state  $s_t$  is replaced with history  $h_t$ . Moreover, as the optimal policy for the last time step  $T$  cannot be obtained directly as in the case of FH-DDPG due to the lack of state information, we need to learn the optimal policy  $\mu_T(h_t)$  by training the actor and critic as well. As a result, a total of  $T$  actors are obtained.

Theoretically, we can use the feed-forward neural networks in DDPG or FH-DDPG for the FH-RDPG algorithm as well. However, it is well-known that recurrent neural networks (RNNs) can learn to preserve information about the past using backpropagation through time (BPTT). Moreover, Long Short-Term Memory Networks (LSTMs) are a type of widely used RNNs that are able to solve shortcomings in the RNN, e.g., vanishing gradient, exploding gradient and long term dependencies, etc.. Therefore, we replace the first feed-forward layers in both the actor and critic networks in FH-DDPG with LSTM layers in the FH-RDPG algorithm. The neural network architectures of the actor and critic in FH-RDPG algorithm are given in Fig. ??.

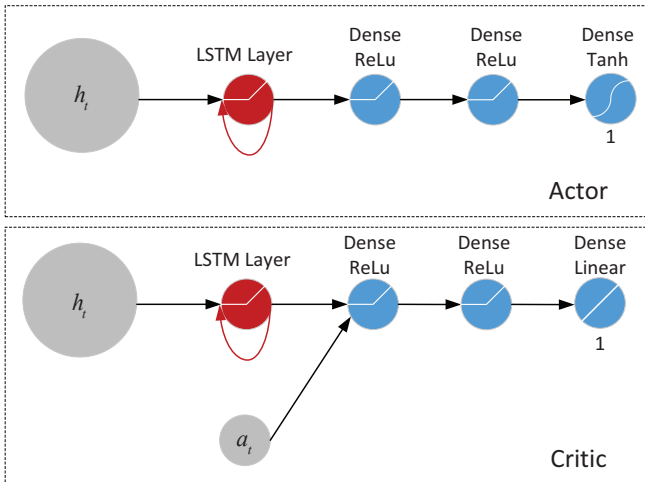


Fig. 2. Actor and Critic Network Architecture of FH-RDPG Algorithm.

### Algorithm 2 FH-RDPG Algorithm

Randomly initialize actor network  $\mu(s|\theta^\mu)$  and critic network  $Q(s, a|\theta^Q)$  with weights  $\theta^\mu = \theta^{\mu 0}$  and  $\theta^Q = \theta^{Q 0}$ . Initialize target networks  $Q'$  and  $\mu'$  with  $\theta^{Q'} \leftarrow \theta^Q$  and  $\theta^{\mu'} \leftarrow \theta^\mu$ .

**for**  $t = T, \dots, 1$  **do**

Initialize replay buffer  $R$

Initialize a random process  $\mathcal{N}$  for action exploration

**for** episode  $e = 1, \dots, M$  **do**

Receive history  $h_t^{(e)}$

Select action  $a_t^{(e)}$  according to the current policy and exploration noise

Execute action  $a_t^{(e)}$  and observe reward  $r_t^{(e)}$  and observe new observation  $o_{t+1}^{(e)}$

Store transition  $(h_t^{(e)}, a_t^{(e)}, r_t^{(e)}, o_{t+1}^{(e)})$  in  $R$

Sample a random minibatch of  $N$  transitions  $(h_t^{(i)}, a_t^{(i)}, r_t^{(i)}, o_{t+1}^{(i)})$  from  $R$

**if**  $t = T$  **then**

Set  $y_T^{(i)} = r_T^{(i)}$

**else**

Construct  $h_{t+1}$  by (9)

Set  $y_t^{(i)} = r_t^{(i)} + \gamma Q'(h_{t+1}^{(i)}, \mu'(h_{t+1}^{(i)}|\theta^{\mu'}))|\theta^{Q'}$

**end if**

Update critic by minimizing the loss:

$$L = \frac{1}{N} \sum_i (y_t^{(i)} - Q(h_t^{(i)}, a_t^{(i)}|\theta^Q))^2$$

Update the actor using the sampled policy gradient:

$$\nabla_{\theta^\mu} J \approx$$

$$\frac{1}{N} \left( \sum_i \nabla_a Q(h_t, a|\theta^Q)|_{h=h_t^{(i)}, a=\mu(h_t^{(i)})} \nabla_{\theta^\mu} \mu(h|\theta^\mu)|_{h_t^{(i)}} \right)$$

**end for**

update the target network:

$$\theta^{Q'} \leftarrow \theta^Q, \theta^{\mu'} \leftarrow \theta^\mu$$

save weight of actor network:

$$\theta^{\mu t} \leftarrow \theta^\mu$$

Reset weight of actor and critic networks to initial value:

$$\theta^Q \leftarrow \theta^{Q 0}, \theta^\mu \leftarrow \theta^{\mu 0}$$

**end for**

### C. Training of the DRL Algorithms

In order to obtain the best performance for a specific day, the DRL algorithms should be trained based on the load and PV data on that day. The obtained policy will be trained to best suit the statistics of that particular day.

However in reality, the load and PV data for the future is not available to train the DRL algorithms. There are generally two methods to address this problem. The first method involves predicting the load and PV data for the future based on the past data, and then train the DRL algorithms using the predicted

data. However, despite the vast amount of existing research for PV and load prediction, the predicted data is still subject to inaccuracies and errors. Therefore, the performance of the first method depends largely on the accuracy of the prediction algorithms.

In the second method, the policy is obtained by training DRL algorithms based on data from the past, and it will be applied for making energy management decisions in the future without knowing the future PV and load data. The advantage of this method is that it learns the policy in one go without depending on the prediction algorithms.

**Remark 3 (Two levels of uncertainty):** In our proposed DRL model, the impact of uncertainty in PV generation and load demand on MG performance is decoupled into two levels. The first level is the “uncertainty for the next time step”, which is captured by the POMDP model. Specifically, the agent can only obtain observation  $o_t = (P_{t-1}^L, P_{t-1}^{PV}, E_t)$  instead of state  $s_t = (P_t^L, P_t^{PV}, E_t)$  at the beginning of time step  $t$ . The second level is the “uncertainty for the next day”, where we train the DRL algorithms using history data to make decisions in the future, where the PV and load statistics are unknown. With the proposed DRL model, we are able to evaluate the impact of both levels of uncertainty on the MG performance in Section V: (1) compare the performance between the MDP and POMDP models to assess the impact of “uncertainty for the next time step”; (2) compare the performance of training and evaluation based on same day data versus different days data to assess the impact of “uncertainty for the next day”.

## V. CASE STUDIES

### A. Experiment Setup

The proposed FH-DDPG and FH-RDPG algorithms are compared with the two baseline DRL algorithms, i.e., DDPG and RDPG algorithms as well as the myopic algorithm under MDP and POMDP environments. The algorithms are trained and evaluated using the real isolated MGs data from Ergon Energy’s 264 kilowatt solar farm at remote Doomadgee in north-west Queensland. The technical constraints and operational parameters of the MG are given in Table I. The parameters involved in the battery model include the maximum charging/discharging power of the battery, the maximum and minimum SoC and charging/discharging efficiency. The operational parameters of the DGs are also summarized in Table I. The interval for each time step is set to  $\Delta t = 1$  hour. Therefore, there are  $T = 24$  time steps in one day. The coefficients in the reward function as given in (10) are set to  $k_1 = 0.001$  and  $k_2 = 1$ , respectively. Moreover, we set  $k_{21} = k_{22} = 1$  in (11).

All the proposed algorithms are implemented in Tensorflow 1.13 which is an open source deep learning platform. Specifically, the parameters for training are summarized in Table II.

### B. Train and evaluate based on same day data

We first train and evaluate the DRL algorithms based on the load and PV data for the same day. The SoC at the beginning of the day is initialized to be a random value. The purpose of the DRL algorithms is to learn the best energy management

TABLE I  
TECHNICAL CONSTRAINTS AND OPERATIONAL PARAMETERS OF THE MG

Battery	$P_{\max}^E$	$E_{\max}$	$E_{\min}$	$\eta_{\text{ch}}$	$\eta_{\text{dis}}$
	120kW	2000kWh	24kWh	0.98	0.98
DG	$P_{\max}^{DG_d}$	$P_{\min}^{DG_d}$	coefficients of cost curve		
			$a_d$	$b_d$	$c_d$
	600kW	100kW	0.005	6	100

TABLE II  
PARAMETERS OF THE DRL ALGORITHMS FOR TRAINING

Parameter	Value
Actor network size	FH-DDPG 400, 300, 100
	FH-RDPG 128, 128, 64
Critic network size	FH-DDPG 400, 300, 100
	FH-RDPG 128, 128, 64
Actor learning rate	5e-6
Critic learning rate	5e-5
History window $\tau$	4
Replay buffer size	20000
Batch size	128
Exploration rate	1
Reward scale	2e-3
Number of training episodes	30000

policy for one specific day from the data. In this case, we can focus on the comparison between the learning capabilities of different DRL algorithms without being affected by the noises due to the statistics discrepancies in different days.

Table III summarizes the performance of two baseline DRL algorithms - DDPG and RDPG, and the performance of our proposed two DRL algorithms - FH-DDPG and FH-RDPG. DDPG and FH-DDPG are evaluated in the MDP environment, where the load and PV data for time step  $t$  are considered to be known at the beginning of time step  $t$ . On the other hand, RDPG and FH-RDPG are evaluated in the POMDP environment, where only the load and PV data for time step  $t - 1$  instead of time step  $t$  are considered to be known at the beginning of time step  $t$ .

In addition to the four DRL algorithms, we also report the performance of the *myopic algorithm* in both the MDP and POMDP environments, where the action  $a_t$  of each time step  $t \in \{1, \dots, T\}$  is selected to optimize the immediate reward  $r_t(s_t, a_t)$  without considering the impact of action  $a_t$  on the future rewards. In POMDP, the myopic algorithm uses observation  $o_t$  in place of  $s_t$  to derive the action.

1) *Returns across 5 runs:* The individual, average, best observed returns as well as the standard error across 5 runs are reported in Table III. For each run, the individual return is obtained by averaging over 100 test episodes after training is completed. Note that the individual returns for the myopic algorithm remain the same across different runs as long as it is in the same environment (i.e., MDP or POMDP). We can observe that for each run, the individual return of the proposed FH-DDPG algorithm is always larger (and thus performance is always better) than those of myopic and DDPG algorithms.



TABLE III  
PERFORMANCE AFTER TRAINING

Environment	Algorithm	Run 1 Return	Run 2 Return	Run 3 Return	Run 4 Return	Run 5 Return	Max Return	Average Return	Std Error
MDP	myopic	-1.1488							0
	DDPG	-0.2817	-0.8986	-8.5000	-1.4037	-0.7835	-0.2817	-2.3734	3.4477
	FH-DDPG	-0.2312	-0.2308	-0.2310	-0.2315	-0.2438	-0.2308	-0.2336	0.0057
POMDP	myopic	-1.5082							0
	RDPG	-0.3887	-0.4344	-0.4474	-0.4179	-0.3299	-0.3299	-0.4036	0.0467
	FH-RDPG	-0.2439	-0.2439	-0.2442	-0.2493	-0.2491	-0.2439	-0.2461	0.0028

The maximum return of FH-DDPG algorithm is larger than those of the myopic and DDPG algorithms by 80% and 18%, respectively. Moreover, the average return of the FH-DDPG algorithm is larger than those of myopic and DDPG algorithms by 80% and 90%, respectively. On the other hand, comparing between DDPG and myopic algorithms, we can observe that the returns of the DDPG algorithm are only larger than those of the myopic algorithm in three out of five runs (when run= 1, 2, 5). Therefore, although the maximum return of the DDPG algorithm is larger than that of the myopic algorithm, the average return of the DDPG algorithm is smaller than that of the myopic algorithm. As shown in Table III, the standard error of the DDPG algorithm is much larger than that of the FH-DDPG algorithm, which indicates that the performance of the proposed FH-DDPG algorithm is much more stable than that of the DDPG algorithm.

Similarly, as can be observed from Table III, we can also observe that for each run, the return of the proposed FH-RDPG algorithm is always larger (and thus performance is always better) than those of myopic and RDPG algorithms. The maximum return of FH-RDPG algorithm is larger than those of myopic and RDPG algorithms by 84% and 26%, respectively. Moreover, the average return of FH-RDPG algorithm is larger than those of myopic and RDPG algorithms by 84% and 39%, respectively. Comparing between RDPG and myopic algorithms, we can observe that the returns of RDPG algorithm are always larger than those of myopic algorithms. This shows that RDPG algorithm is relatively stable in the considered microgrid environment. However, FH-RDPG algorithm is even more stable than the RDPG algorithm, as the standard error of FH-RDPG is smaller than that of RDPG.

We can also observe from Table III that the returns of FH-DDPG algorithm are always larger than those of FH-RDPG algorithm. This is due to the fact that FH-DDPG is run in the MDP environment, where the state information is available to the agent for selecting actions; while FH-RDPG algorithm is run in the POMDP environment, which considers the practical scenario that only the observation information is available to the agent. The average return of FH-RDPG is smaller than that of FH-DDPG by 5%. This performance loss of FH-RDPG over FH-DDPG is due to the “uncertainty for the next time step” as discussed in Remark 3. On the other hand, the average return of myopic algorithm in POMDP environment is smaller than that in MDP environment by 31%. This observation indicates that the FH-RDPG algorithm exploits the history data to make

more efficient decisions as compared to the myopic algorithm.

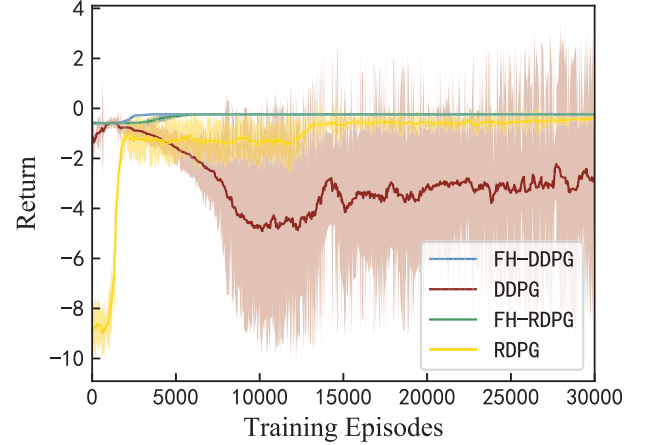


Fig. 3. Performance curves for the four DRL algorithms.

2) *Convergence properties:* The policies are evaluated periodically during training without noise. The performance curves for the four DRL algorithms are given in Fig. 3, where the vertical axis corresponds to the average return across 5 runs and the shaded areas indicate the standard errors of the four algorithms. For FH-DDPG and FH-RDPG algorithms, we only show the performance curve of the first time step  $t = 1$  due to space limitation in this paper, as the performance curves for all  $T - 1$  (for FH-DDPG) or  $T$  (for FH-RDPG) time steps are similar, except that the returns grow more and more negative with decreasing time steps. Fig.3 shows that both FH-DDPG and FH-RDPG learn much faster than DDPG and RDPG algorithms. This is due to the fact that FH-DDPG and FH-RDPG algorithms are designed to iteratively train to solve the one-period MDP and POMDP problems with two time steps, which are much easier to converge than the finite-horizon MDP and POMDP problems with  $T$  time steps faced by DDPG and RDPG algorithms. Moreover, it can also be observed from Fig.3 that the shaded areas of both FH-DDPG and FH-RDPG algorithms are much smaller than those of the DDPG and RDPG algorithms, indicating that the proposed algorithms perform stably across different runs.

3) *Accuracy of  $Q$ -values estimations:* As learning accurate  $Q$ -values is very important for the success of actor-critic algorithms, we examined the  $Q$ -values estimated by the critic after training for all the four DRL algorithms by comparing



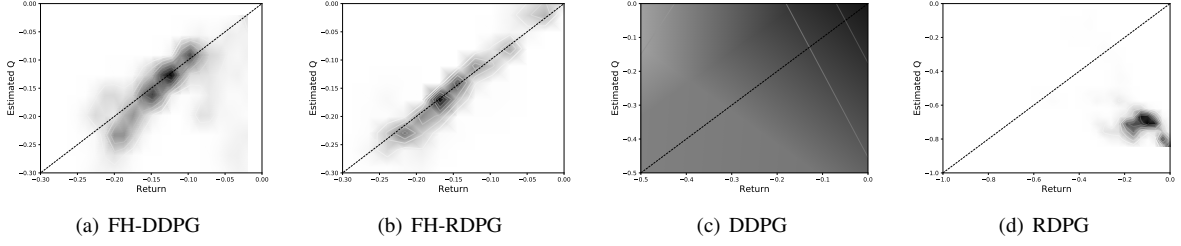


Fig. 4. Density plot showing estimated Q values versus observed returns from test episodes on 5 runs.

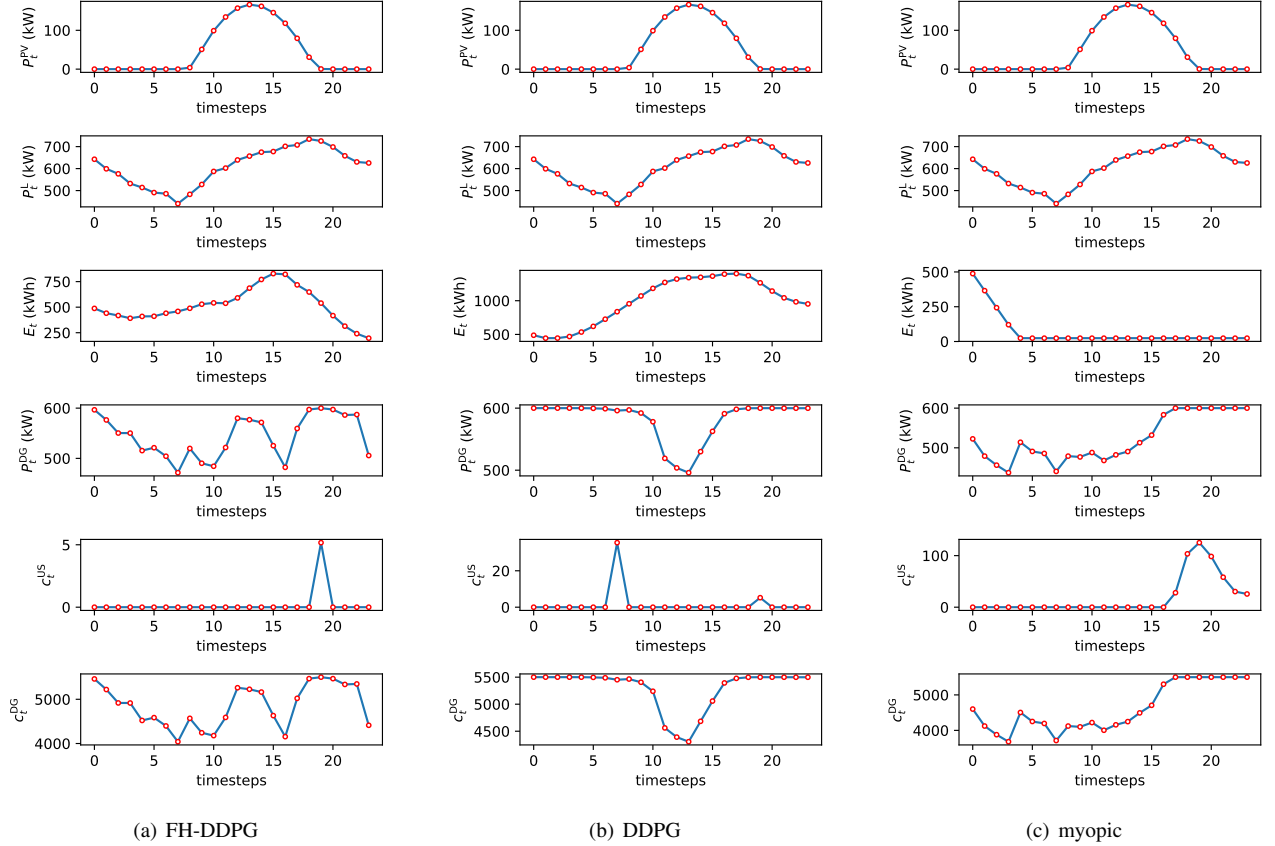


Fig. 5. Energy dispatch results for a specific test episode under the MDP environment.

them with the true returns seen on the test episodes. Fig. 4(a) and Fig. 4(b) show that both FH-DDPG and FH-RDPG algorithms can provide accurate estimation of Q-values. On the other hand, Fig. 4(d) shows that the estimated Q-values of RDPG have a systematic bias that make the estimated Q-values deviate from the true returns. Finally, Fig. 4(c) demonstrates that the estimated Q-values of DDPG cannot reflect the true returns at all. This is because for the five runs, only Run 1 converges while all the other four runs fail.

4) *Energy dispatch results:* In order to obtain insights for the design of energy dispatch policies, we focus on a specific test episode corresponding to one day, and plot the energy dispatch results  $P_t^{DG}$  along with the immediate DG generation cost  $c_t^{DG}$  and power unbalance cost  $c_t^{US}$  as well as PV and load data for all the time steps  $t \in \{1, 2, \dots, 24\}$ . Fig. 5 shows the results for FH-DDPG, DDPG, and myopic algorithms under

the MDP environment. The day starts at 12 : 00 AM midnight, when the PV generation is zero. The PV output power starts to increase from 8 : 00 AM until it reaches the peak value at around 2 : 00 PM. The load decreases from midnight till around 7 : 00 AM in the morning, and starts to increase until the peak value is reached at 6 : 00 PM. The initial SoC of battery is 500kWh.

As we can see in Fig. 5(a), in the energy dispatch policy obtained by the FH-DDPG algorithm, the DG output power first tracks the load demand so that the SoC of the battery remains almost constant. After the PV generation starts to increase after 8 : 00 AM, the DG power output slowly charges the battery so that the SoC increases to 750kWh. This is very important, as when the load demand reaches the peak value at 6 : 00 PM later that day, the PV power generation is no longer available, and the maximum DG output power is not enough

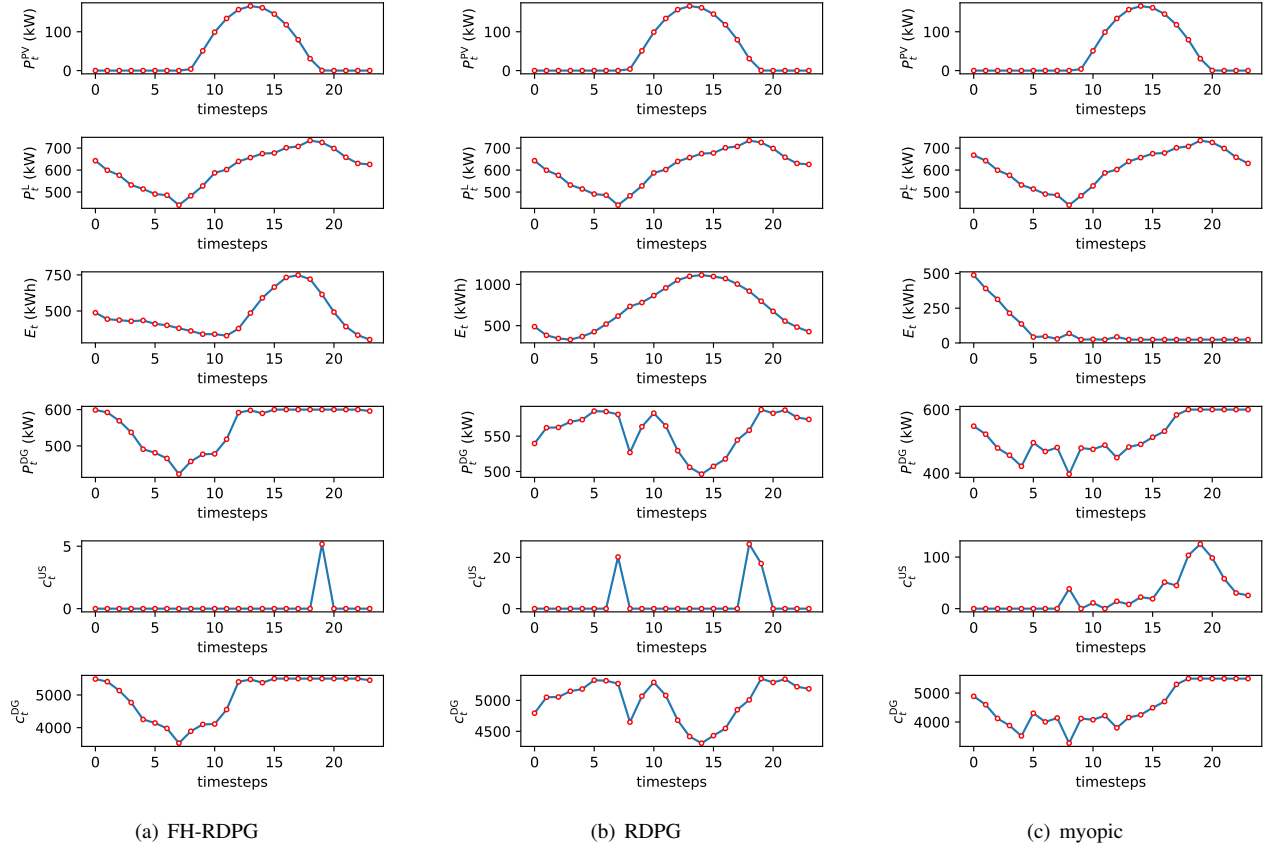


Fig. 6. Energy dispatch results for a specific test episode under the POMDP environment.

to meet the large load demand. In this case, the battery can discharge to maintain the power supply and demand balance. As a result, the cost of power unbalance  $c_t^{US}$  is always 0 except for time step 19. Moreover, note that little DG output power is wasted to charge up the battery, as the SoC of the battery at the end of the day is at a low level. Therefore, DG generation cost  $c_t^{DG}$  is also low.

On the other hand, as can be observed from Fig. 5(c), the myopic algorithm quickly discharges the battery energy at the beginning of the day in order to save DG output power, without considering that the DG output power will not be able to meet load demand later that day. This results in that the cost of power unbalance  $c_t^{US}$  is not 0 after 4 : 00 PM. In contrast, DDPG algorithm begins to charge up the battery at the beginning of the day as shown in Fig. 5(b). Although the battery can help to maintain power balance in this case, the DG output power is wasted as the SoC of battery is quite high at the end of the day, resulting in large DG power generation cost  $c_t^{DG}$ .

Fig. 6 shows the results for FH-RDPG, RDPG, and myopic algorithms under the POMDP environment. As can be observed in Fig. 6(a) and Fig. 6(b), both FH-RDPG and RDPG, algorithms charge the battery before the peak hour for the loads similar to FH-DDPG and DDPG algorithms, so that they can avoid power unbalance in most time steps. On the other hand, the myopic algorithm under POMDP environment discharges the battery from the beginning of the day similar

to its behaviour under MDP environment, which results in power unbalance later that day. FH-RDPG algorithm keeps the power balanced, i.e.,  $c_t^{US} = 0$ , in more time steps than RDPG algorithm. On the other hand, the SoC of battery at the end of day for both FH-RDPG and RDPG algorithms are larger than that of FH-DDPG algorithm, resulting in larger DG power generation cost  $c_t^{DG}$ .

### C. Train and evaluate based on history data

In order to achieve a good performance, the trained policy based on past data needs to be general enough to adapt to the unknown situation in the future. Therefore, we need to train the DRL algorithms based on the past data in multiple days to prevent the learned policy from over-fitting to the statistics of one particular day. However, a policy that is too general may result in poor performance for all the days no matter in the past or future. Therefore, the number of days to train the DRL algorithms is an important parameter that will affect the performance results.

We report the average returns of the four DRL algorithms across 5 runs where the policies are trained based on the load and PV data of past 7, 14, and 21 days, respectively. Fig. 7 and Fig. 8 show the results when the trained policies are tested on the next day in MDP and POMDP environments, respectively. It can be observed that the proposed FH-DDPG and FH-RDPG algorithms (yellow bars) still outperform the baseline DDPG and RDPG algorithms (red bars) by a large

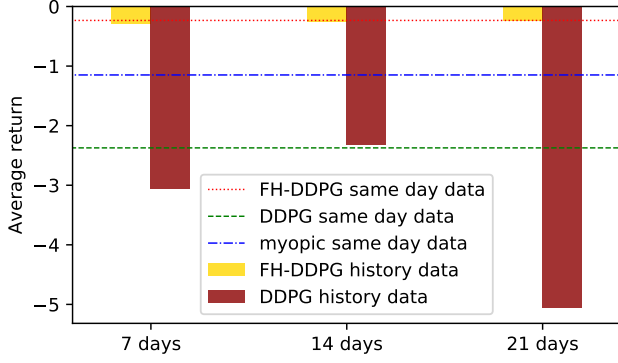


Fig. 7. Average returns of FH-DDPG and DDPG when trained based on history data and same day data.

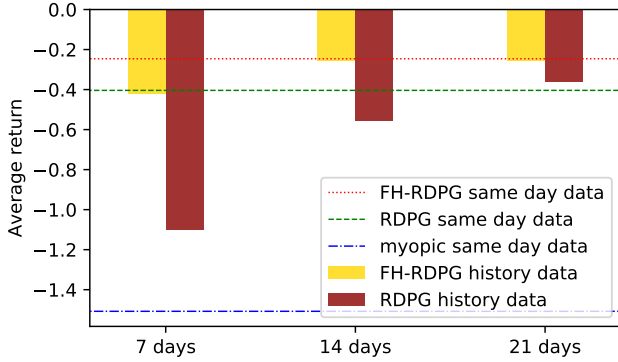


Fig. 8. Average returns of FH-RDPG and RDPG when trained based on history data and same day data.

margin when trained based on history data. Moreover, the number of days to train the DRL algorithms has a larger impact on DDPG and RDPG algorithm than on FH-DDPG and FH-RDPG algorithms.

We also compare the above results with those in Table III, where the policies are trained based on the same day data instead of history data. For comparison purpose, we plot the results in Table III by dashed and dotted lines in Fig. 7 and Fig. 8. It can be observed that the performance of FH-DDPG and FH-RDPG are quite similar when trained based on history data and same day data. This is also true for DDPG and RDPG algorithms. This result shows that the DRL algorithms can cope well with the “uncertainty for the next day” as discussed in Remark 3.

## VI. CONCLUSION

This paper studied DRL-based dynamic energy dispatch methods for isolated MG. Firstly, a finite-horizon MDP model and a finite-horizon POMDP model were formulated for energy dispatch, respectively. Then, considering the characteristics of finite-horizon setting, FH-DDPG and FH-RDPG algorithms were proposed to provide better stability performance over the baseline DRL algorithms under MDP and POMDP models, respectively. Finally, the performance of FH-DDPG and FH-RDPG algorithms were compared with DDPG,

RDPG and myopic algorithms based on real same day data and history data in MG. The results show that our proposed algorithms have derived better energy dispatch policies for both MDP and POMDP models. Moreover, by comparing between FH-DDPG and FH-RDPG algorithms, as well as the results of training with same day data and history data, we quantified the impact of uncertainty on system performance. We have also demonstrated that the FH-RDPG algorithm can make efficient decisions when only partial state information is available as in most practical scenarios. Our future work involves the joint optimization of unit commitment and energy dispatch of multiple DGs in isolated MGs.

## REFERENCES

- [1] W. Su, J. Wang, and J. Roh, “Stochastic energy scheduling in microgrids with intermittent renewable energy resources,” *IEEE Transactions on Smart Grid*, vol. 5, no. 4, pp. 1876–1883, Jul. 2014.
- [2] Z. Wang, B. Chen, J. Wang, M. M. Begovic, and C. Chen, “Coordinated energy management of networked microgrids in distribution systems,” *IEEE Transactions on Smart Grid*, vol. 6, no. 1, pp. 45–53, Jan. 2015.
- [3] H. Farzin, M. Fotuhi-Firuzabad, and M. Moeini-Aghaie, “A stochastic multi-objective framework for optimal scheduling of energy storage systems in microgrids,” *IEEE Transactions on Smart Grid*, vol. 8, no. 1, pp. 117–127, Jan. 2017.
- [4] Y. Zhang, N. Gatsis, and G. B. Giannakis, “Robust energy management for microgrids with high-penetration renewables,” *IEEE Transactions on Sustainable Energy*, vol. 4, no. 4, pp. 944–953, Oct. 2013.
- [5] J. S. Giraldo, J. A. Castrillon, J. C. Lpez, M. J. Rider, and C. A. Castro, “Microgrids energy management using robust convex programming,” *IEEE Transactions on Smart Grid*, vol. 10, no. 4, pp. 4520–4530, Jul. 2019.
- [6] D. E. Olivares, C. A. Caizares, and M. Kazerani, “A centralized energy management system for isolated microgrids,” *IEEE Transactions on Smart Grid*, vol. 5, no. 4, pp. 1864–1875, Jul. 2014.
- [7] D. Zhu and G. Hug, “Decomposed stochastic model predictive control for optimal dispatch of storage and generation,” *IEEE Transactions on Smart Grid*, vol. 5, no. 4, pp. 2044–2053, Jul. 2014.
- [8] J. Sachs and O. Sawodny, “A two-stage model predictive control strategy for economic diesel-PV-battery island microgrid operation in rural areas,” *IEEE Transactions on Sustainable Energy*, vol. 7, no. 3, pp. 903–913, Jul. 2016.
- [9] J. D. Lara, D. E. Olivares, and C. A. Caizares, “Robust energy management of isolated microgrids,” *IEEE Systems Journal*, vol. 13, no. 1, pp. 680–691, Mar. 2019.
- [10] P. Zeng, H. Li, H. He, and S. Li, “Dynamic energy management of a microgrid using approximate dynamic programming and deep recurrent neural network learning,” *IEEE Transactions on Smart Grid*, 2018.
- [11] H. Shuai, J. Fang, X. Ai, J. Wen, and H. He, “Optimal real-time operation strategy for microgrid: An adp-based stochastic nonlinear optimization approach,” *IEEE Transactions on Sustainable Energy*, vol. 10, no. 2, pp. 931–942, 2018.
- [12] H. Shuai, J. Fang, X. Ai, Y. Tang, J. Wen, and H. He, “Stochastic optimization of economic dispatch for microgrid based on approximate dynamic programming,” *IEEE Transactions on Smart Grid*, vol. 10, no. 3, pp. 2440–2452, May 2019.
- [13] W. Shi, N. Li, C. Chu, and R. Gadh, “Real-time energy management in microgrids,” *IEEE Transactions on Smart Grid*, vol. 8, no. 1, pp. 228–238, Jan. 2017.
- [14] W. Hu, P. Wang, and H. B. Gooi, “Toward optimal energy management of microgrids via robust two-stage optimization,” *IEEE Transactions on Smart Grid*, vol. 9, no. 2, pp. 1161–1174, Mar. 2018.
- [15] Q. Zheng, K. Zheng, H. Zhang, and V. C. M. Leung, “Delay-optimal virtualized radio resource scheduling in software-defined vehicular networks via stochastic learning,” *IEEE Transactions on Vehicular Technology*, vol. 65, no. 10, pp. 7857–7867, Oct. 2016.
- [16] L. Lei, Y. Tan, S. Liu, K. Zheng, and X. Shen, “Deep reinforcement learning for autonomous internet of things: Model, applications and challenges,” *arXiv preprint arXiv:1907.09059*, 2019.
- [17] V. Mnih, K. Kavukcuoglu, D. Silver, A. A. Rusu, J. Veness, M. G. Bellemare, A. Graves, M. Riedmiller, A. K. Fidjeland, G. Ostrovski et al., “Human-level control through deep reinforcement learning,” *Nature*, vol. 518, no. 7540, p. 529, 2015.

- [18] H. Van Hasselt, A. Guez, and D. Silver, "Deep reinforcement learning with double Q-learning," in *Thirtieth AAAI Conference on Artificial Intelligence*, 2016.
- [19] R. J. Williams, "Simple statistical gradient-following algorithms for connectionist reinforcement learning," *Machine learning*, vol. 8, pp. 229–256, 1992.
- [20] T. P. Lillicrap, J. J. Hunt, A. Pritzel, N. Heess, T. Erez, Y. Tassa, D. Silver, and D. Wierstra, "Continuous control with deep reinforcement learning," *arXiv preprint arXiv:1509.02971*, 2015.
- [21] V. Mnih, A. P. Badia, M. Mirza, A. Graves, T. Lillicrap, T. Harley, D. Silver, and K. Kavukcuoglu, "Asynchronous methods for deep reinforcement learning," in *International conference on machine learning*, 2016, pp. 1928–1937.
- [22] J. Schulman, S. Levine, P. Abbeel, M. Jordan, and P. Moritz, "Trust region policy optimization," in *International Conference on Machine Learning*, 2015, pp. 1889–1897.
- [23] N. Heess, J. J. Hunt, T. P. Lillicrap, and D. Silver, "Memory-based control with recurrent neural networks," *arXiv preprint arXiv:1512.04455*, 2015.
- [24] V. François-Lavet, D. Taralla, D. Ernst, and R. Fonteneau, "Deep reinforcement learning solutions for energy microgrids management," in *European Workshop on Reinforcement Learning (EWRL 2016)*, 2016.
- [25] G. K. Venayagamoorthy, R. K. Sharma, P. K. Gautam, and A. Ahmadi, "Dynamic energy management system for a smart microgrid," *IEEE transactions on neural networks and learning systems*, vol. 27, no. 8, pp. 1643–1656, 2016.
- [26] E. Foruzan, L. Soh, and S. Asgarpour, "Reinforcement learning approach for optimal distributed energy management in a microgrid," *IEEE Transactions on Power Systems*, vol. 33, no. 5, pp. 5749–5758, Sep. 2018.
- [27] L. Yu, W. Xie, D. Xie, Y. Zou, D. Zhang, Z. Sun, L. Zhang, Y. Zhang, and T. Jiang, "Deep reinforcement learning for smart home energy management," *IEEE Internet of Things Journal*, 2019.
- [28] M. S. Munir, S. F. Abedin, N. H. Tran, and C. S. Hong, "When edge computing meets microgrid: A deep reinforcement learning approach," *IEEE Internet of Things Journal*, vol. 6, no. 5, pp. 7360–7374, 2019.
- [29] A. Irpan, "Deep reinforcement learning doesn't work yet," <https://www.alexirpan.com/2018/02/14/rl-hard.html>, 2018.
- [30] M. L. Puterman, *Markov Decision Processes.: Discrete Stochastic Dynamic Programming*. John Wiley & Sons, 2014.
- [31] I. Grondman, H. Xu, S. Jagannathan, and R. Babuška, "Solutions to finite horizon cost problems using actor-critic reinforcement learning," in *The 2013 International Joint Conference on Neural Networks (IJCNN)*. IEEE, 2013, pp. 1–7.